Model to Describe Fast Shutoff of CoVID-19 Pandemic Spread

Genghmun Eng
PhD Physics 1978, University of Illinois at Urbana-Champaign
geng001@socal.rr.com

August 6, 2020

Abstract

Early CoVID-19 growth obeys: $N\{\widehat{t}\} = N_I \exp[+K_o\,\widehat{t}\,]$, with $K_o = [(\ln 2)/(t_{dbl})]$, where t_{dbl} is the pandemic growth *doubling time*. Given $N\{\widehat{t}\}$, the daily number of new CoVID-19 cases is $\rho\{\widehat{t}\} = dN\{\widehat{t}\}/d\widehat{t}$. Implementing society-wide *Social Distancing* increases the t_{dbl} *doubling time*, and a linear function of time for t_{dbl} was used in our *Initial Model*:

$$N_o[t] = \mathbf{1}\,\exp[+K_A t/(1+\gamma_o t)] \equiv e^{+G_o}\,\exp(-Z_o[t]),$$

to describe these changes, with $G_o \equiv [K_A/\gamma_o]$. However, this equation could not easily model some quickly decreasing $\rho[t]$ cases, indicating that a second *Social Distancing* process was involved. This second process is most evident in the initial CoVID-19 data from *China*, *South Korea*, and *Italy*. The *Italy* data is analyzed here in detail as representative of this second process. Modifying $Z_o[t]$ to allow exponential cutoffs:

$$Z_E[t] \equiv +[G_o\,/\,(1+\gamma_o\,t)]\,[\exp(-\delta_o t - q_o t^2)] = Z_o[t]\exp(-\delta_o t - q_o t^2),$$

provides a new *Enhanced Initial Model (EIM)*, which significantly improves datafits, where $N_E[t] = e^{+G_o}\,\exp(-Z_E[t])$. Since large variations are present in $\rho_{data}[t]$, these models were generalized into an orthogonal function series, to provide additional data fitting parameters:

$$N(Z) = \sum_{m=0}^{m=M_F} g_m\,L_m(Z)\,\exp[-Z]\,.$$

Its first term can give $N_o[t]$ or $N_E[t]$, for $Z[t] \to Z_o[t]$ or $Z[t] \to Z_E[t]$. The $L_m(Z)$ are *Laguerre Polynomials*, with $L_0(Z) = 1$, and $\{g_m;\, m = 0, M_F\}$ are constants derived from each dataset. When $\rho[t] = dN[t]/dt$ gradually decreases, using $Z_o[t]$ provided good datafits at small M_F values, but was inadequate if $\rho[t]$ decreased faster. For those cases, $Z_E[t]$ was used in the above $N(Z)$ series to give the most general *Enhanced Orthogonal Function [EOF]* model developed here. Even with $M_F = 0$, $q_o = 0$, this *EOF* model fit the *Italy* CoVID-19 data for $\rho[t] \equiv dN[t]/dt$ fairly well.

When the $\rho[t]$ post-peak behavior is not Gaussian, then $Z_E[t]$ with $\delta_o \neq 0$, $q_o = 0$; which we call $Z_A[t]$, is also likely to be a sufficient extension of the $Z_o[t]$ model. The *EOF* model also can model a gradually decreasing $\rho[t]$ tail using small $\{\delta_o, q_o\}$ values [with *6 Figures*].

1 Introduction

Let $N\{\widehat{t}\}$ be the total number of CoVID-19 cases in any given locality, with $\rho\{\widehat{t}\}$ being the predicted number of daily new CoVID-19 cases, so that:

$$N\{\widehat{t}\} = \int_{t'=0}^{t'=\widehat{t}} \rho\{t'\}\, dt' \,, \qquad [1.1a]$$

$$\rho\{\widehat{t}\} = dN\{\widehat{t}\} \,/\, d\widehat{t} \,. \qquad [1.1b]$$

Early CoVID-19 growth often obeys $N\{\widehat{t}\} \approx N_I \exp[+K_o\, \widehat{t}\,]$, with $K_o = [(\ln 2)/t_{dbl}]$, where t_{dbl} is the pandemic *doubling time*. The start of society-wide *Social Distancing* at $\widehat{t} = 0$ can gradually lengthen t_{dbl} for $\widehat{t} > 0$. The $\widehat{t} < 0$ exponential growth phase is not applicable for estimating *Social Distancing* effects. For $\widehat{t} > 0$, an *Initial Model* for CoVID-19 pandemic shutoff was first developed[1] using a linear function of time to describe the t_{dbl} changes:

$$N\{\widehat{t}\} = N_I \exp[+K_o\, \widehat{t}\,/\,(1 + \alpha_S\, \widehat{t})] \,. \qquad [1.2]$$

Given measured $N_{data}\{\widehat{t}\}$, the data end-points $\{N_I,\, N_F\}$ help to set $\{K_o,\, \alpha_S\}$. An *Orthogonal Function Model [OFM]* was developed next[2], with Eq. [1.2] as the first term of the orthogonal function series. Each new *OFM* term provides another fitting parameter, to progressively better match $N_{data}\{\widehat{t}\}$ and $\rho_{data}\{\widehat{t}\} = (d/d\widehat{t})\, N_{data}\{\widehat{t}\}$.

The *OFM* improves on the *Initial Model*, and it works best with gradually decreasing $\rho\{\widehat{t}\}$ ["*Slow Shutoff*"]. In contrast, when $\rho\{\widehat{t}\}$ decreased quickly ["*Fast Shutoff*"], the *Initial Model* was not a good datafit, and a few-term *OFM* series only gave small improvements. This result indicates there is an inherent limit to what the gradually changing t_{dbl} *doubling time* of Eq. [1.2] can model.

For these cases, typified by CoVID-19 pandemic evolution in Italy, data often showed a stage where $\rho_{data}\{\widehat{t}\} \sim [\exp(-\delta_o \widehat{t})]$ or $\rho_{data}\{\widehat{t}\} \sim [\exp(-q_o \widehat{t}^{\,2})]$, which likely represents a second process, independent of the gradually changing t_{dbl} *doubling time*. An *Enhanced Initial Model (EIM)* is developed here to include this second process. The prior *OFM* methods can then be applied, giving an *Enhanced Orthogonal Function (EOF)* model for this more general case.

1.1 Review of Prior Models

The *Initial Model* of Eq. [1.2] is still needed as the first part of the *OFM*. The *Initial Model* starts with measured data end-points $\{N_I,\, N_F\}$, where $\widehat{t} = (t_F - t_I)$ is the largest data time interval so that $N\{\widehat{t} = (t_F - t_I)\} = N_F$. Usually α_S in Eq. [1.2] was chosen first, and K_o or t_{dbl} adjusted to match the N_F data end-point, using an *Excel*^{TM}*_Goal-Seek* or its equivalent. The final $\{K_o,\, \alpha_S\}$ values were the pair with the minimum *root-mean-square* (*rms*) error between the given data and the Eq. [1.2] model.

The above $\{K_o,\, \alpha_S\}$ also provides a $t = 0$ estimate for the pandemic start, and gives $\{K_A,\, \gamma_o\}$ as new data fitting parameters:

$$N_o[t] = \mathbf{1} \exp[+K_A\, t\,/\,(1 + \gamma_o\, t)] \equiv \exp[+G_o] \exp(-Z_o[t]) \,, \qquad [1.3a]$$

$$G_o \equiv (K_A\,/\,\gamma_o) \,, \qquad [1.3b]$$

$$Z_o[t] = +[G_o\,/\,(1 + \gamma_o\, t)] \,, \qquad [1.3c]$$

$$\rho_o[t] \equiv dN_o[t] \,/\, dt\,. \qquad [1.3d]$$

Using $(t_F - t_I)$, with $N_o[t = t_I] = N_I$ and $N_o[t = t_F] = N_F$, sets:

$$t_I \;= \ln(N_I) \,/ [K_o + \alpha_S \,\ln(N_I)]\,. \qquad [1.4a]$$

$$t_F \;= \ln(N_I) \,/ [K_o + \alpha_S \,\ln(N_I)] + (t_F - t_I)\,, \qquad [1.4b]$$

which determines $\{K_A,\, \gamma_o\}$ in $Z_o[t]$ for Eq. [1.3c]:

$$\gamma_o = \{\,[\ln(N_I) \,/\, t_I] - [\ln(N_F) \,/\, t_F]\,\} \,/\, [\,\ln(N_F) - \ln(N_I)\,]\,, \qquad [1.5a]$$

$$K_A = [\,(1 \,/\, t_I) - (1 \,/\, t_F)\,] \,/\, \{\,[1 \,/\, \ln(N_I)] - [1 \,/\, \ln(N_F)]\,\}\,. \qquad [1.5b]$$

The Eq. [1.4a] value for t_I is what determines the new $t = 0$ point, as an extrapolation for when $N_o[t = 0] = \mathbf{1}$. In addition:

$$N_o[t \to \infty,\; Z_o \to 0] \approx \mathbf{1}\, \exp[+K_A \,/\, \gamma_o] \;= \exp[+G_o] \equiv N^o_{\max}\,, \qquad [1.6a]$$

$$\rho_o[t] = dN_o[t] \,/\, dt \approx N_o[t]\,[G_o\,\gamma_o \,/\, (1 + \gamma_o\, t)^2] \;\to N^o_{\max}\,[G_o \,/\, (\gamma_o\, t^2)]\,, \qquad [1.6b]$$

provides an estimate for the total number of cases ($N^o_{\max}$) at the pandemic end, and determines a function for the $\rho_o[t]$ long-time tail. The $\{0 < t < t_I\}$ period prior to the start of *Social Distancing*, extrapolates what pandemic progress would have looked like, if *Social Distancing* had begun at $t = 0$.

An *Orthogonal Function Model [OFM]* was then developed[2] to better model the different observed $\rho_{data}[t]$ shapes, as an improvement of the *Initial Model*:

$$N(Z) = \sum_{m=0}^{m=M_F} g_m\, L_m(Z)\, \exp[-Z]\,, \qquad [1.7a]$$

$$R(Z) = \sum_{m=0}^{m=M_F} c_m\, L_m(Z)\, \exp[-Z]\,, \qquad [1.7b]$$

$$N(Z) \equiv \int_{Z'=Z}^{Z'=+\infty} R(Z')\, d\, Z', \qquad [1.7c]$$

$$c_{M_F - k} = \sum_{m=0}^{m=k} g_m\,, \qquad [1.7d]$$

with $L_m(Z)$ being the *Laguerre Polynomials*, and $L_m(Z = 0) = L_0(Z) \equiv 1$. Using $Z = Z_o[t]$ from Eq. [1.3c] gives $N(Z) \to N(Z_o)$ and $R(Z) \to R(Z_o)$.

The $\{g_m;\; m = (0, M_F)\}$ constants in Eq. [1.7a] can be arranged in a $\overrightarrow{g}-$vector form, with comparable constants for $R(Z)$ from Eq. [1.7b] arranged in a $\overrightarrow{C}-$vector form. For $M_F = 2$, it allows Eq. [1.7d] to be written as:

$$\overrightarrow{C} \;= \begin{pmatrix} c_0 \\ c_1 \\ c_2 \end{pmatrix} = \begin{pmatrix} 1 & 1 & 1 \\ 0 & 1 & 1 \\ 0 & 0 & 1 \end{pmatrix} \overrightarrow{g} = \begin{pmatrix} 1 & 1 & 1 \\ 0 & 1 & 1 \\ 0 & 0 & 1 \end{pmatrix} \begin{pmatrix} g_0 \\ g_1 \\ g_2 \end{pmatrix}. \qquad [1.8]$$

Once these c_m values are determined for $R(Z)$ in Eqs. [1.7b]-[1.7c], an *OFM* feature is that c_0, by itself, becomes the *OFM* best estimate for the total number of CoVID-19 cases at the pandemic end.

For large enough M_F values, and a monotonic $Z-$function, this *OFM* can provide successively better approximations to almost any given set of $N_{data}[Z]$, with $Z[t] \to Z_o[t]$ of Eq. [1.3c] being a specific case.

The *OFM* implicitly uses a *Linear Y-axis*, so its results differ from the *Initial Model* datafit on a *Logarithmic Y-axis*. As an example, compare the *Initial Model* result of $N_o(Z_o) = G_0\, \exp[-Z_o]$ with the Eq. [1.7a] *OFM* result of $N(Z_o) = g_0\, \exp[-Z_o]$ for $M_F = 0$. In the *Initial Model*, G_o is fixed so that $N_o(Z_o)$ exactly matches $\{N_I,\, N_F\}$ at the $\{t_I,\, t_F\}$ boundaries. In the *OFM*,

$g_0 = G_o$ is no longer required, so that the *OFM* $N(Z_o)$ best datafit is not constrained to exactly match $\{N_I,\, N_F\}$ at $\{t_I,\, t_F\}$.

The above $R(Z)$ and $Z[t]$ gives $N[t]$ and $\rho[t]$ as an explicit functions of time:

$$N[t] \equiv \int_{\widehat{z}=Z[t],\ t'=t}^{\widehat{z}=+\infty,\ t'=(t_{\min})} R(Z[t'])\,\tfrac{dZ}{dt'}\,d\,t' \equiv \int_{t'=(t_{\min})}^{t'=t} \rho[t']\,dt' \,. \qquad [1.9]$$

Since Eq. [1.6b] gives $\rho\{t\} \sim [1/t^2]$, the aim here is to model faster decaying functions such as $\rho\{t\} \sim [\exp(-\delta_o t)]$ or $\rho\{t\} \sim [\exp(-q_o t^2)]$.

1.2 Updated *Initial Model* Results for Italy

The $Z_o[t]$ model of Eq. [1.3a] was applied to *bing.com* data[9] for Italy, starting with $N_{data}^{2/23/2020} = 150$ CoVID-19 cases as an early pandemic point, up through June 15, 2020. Here, t_I is when mandatory *Social Distancing* was introduced at $N_{data}^{3/10/2020} = 10,149$; with t_F being when $N_{data}^{6/15/2020} = 237,290$. Data prior to *Social Distancing* ($t < t_I$) was excluding from this *Social Distancing* analysis.

Figure 1 compares the $\rho_{data}[t]$ results with the updated $N_o[t]$ and $\rho_o[t] = dN_o[t]/dt$ predictions using $Z_o[t]$. The $N_{data}^{2/23/2020}$ (*Day* 1) to $N_{data}^{3/10/2020}$ (*Day* 17) interval was examined for estimating a $t = 0$ pandemic start where $N_{data}[t = 0] \to \mathbf{1}$. A best fit value of $t_{offset} = 9.10055\,days$ was found, giving $t_I = (17 - 9.10055) = 8.89945\,days$ for $N_{data}^{3/10/2020}$ (*Day* 17), while $N_{data}^{6/15/2020}$ (*Day* 114) gives $t_F = (114 - 9.10055) = 104.89945\,days$, so that:

$$N_{data}[t_I = 8.899] = 10,149\,; \qquad [1.10a]$$
$$N_{data}[t_F = 104.899] = 237,290\,; \qquad [1.10b]$$
$$N_{data}^{3/2/2020}[t = 0] = \mathbf{1}\,, \qquad [1.10c]$$
$$N[t \to \infty] = 338,165\,; \qquad [1.10d]$$

with $\{K_A,\, \gamma_o\} \approx \{4.2405,\, 0.33078\}$ and $(t_F - t_I) = 97\,days$. In **Fig. 1**, the X-axis uses this $t = 0$ point where $N_o[t = 0] \to \mathbf{1}$, and it shows what *Social Distancing* effects would have been, if it had been operating throughout the $t > 0$ period. This $\rho_o[t]$ prediction still has a much more gradual drop than the data. This discrepancy indicates that a second *Social Distancing* process is operating, besides just the gradual t_{dbl} lengthening of the *Initial Model*.

Figure 2 compares the $N_o[t]$ predictions for this model, to the measured $N_{data}[t]$. Systematic deviations are evident, with the net *rms* error on a *Logarithmic Y-axis* being $rms_{error} = 0.097828$. To cure these defects, an enhanced $Z[t]$ model is developed next.

2 Developing Enhanced $Z[t]$ Models

To generalize $Z[t]$ beyond Eq. [1.3c], it is convenient to use the $t = \{0^+, \infty^-\}$ domain, and require convergence of $Z[t] \to Z_o[t]$ in some limit, along with:

$$\lim_{t \to 0}\{Z[t]\} = G_o \equiv [K_A\,/\,\gamma_o]\,, \qquad [2.1a]$$
$$\lim_{t \to +\infty}\{Z[t]\} = 0\,, \qquad [2.1b]$$

and that the $M_F = 0$ case of Eq. [1.7a] remains as:

$$N(Z) = g_0 \, \exp[-Z] \, . \qquad [2.2]$$

How to choose an appropriate $Z[t]$, as part of an *Enhanced Initial Model* (*EIM*), which also allows a $\rho[t] \sim [\exp(-\delta_o t)]$ or $\rho[t] \sim [\exp(-q_o t^2)]$ stage, is examined next. It can be motivated by studying a simple $N_T[t]$ test-case, where $\rho_T[t]$ itself is a pure exponential decay, as a function of time:

$$N_T[t] = [e^{+G_o}] \, [(1 + e^{-G_o}) - \exp(-\delta_o t)] \, , \qquad [2.3a]$$

$$\rho_T[t] = \{dN_T[t] \, / \, dt\} = [\delta_o \, e^{+G_o}] \, \exp(-\delta_o t), \qquad [2.3b]$$

while also preserving $N_T\{t \to 0\} = 1$. Comparing Eq. [2.3a] to the Eq. [2.2], sets $Z_T[t]$ for this test-case:

$$N_T[t] = \exp[+G_o] \, \exp(-Z_T[t]) \, , \qquad [2.4a]$$

$$Z_T[t] = (-1) \, \ln \, [(1 + e^{-G_o}) - \exp(-\delta_o t)] \, . \qquad [2.4b]$$

At large times, Eq. [2.4b] gives:

$$\lim_{t \to \infty} \{Z_T[t]\} \approx \exp(-\delta_o t), \qquad [2.5]$$

since $(-\ln[1 - x] \approx x)$ for small x, which shows that if $\rho_T[t]$ has an exponential tail, then $Z_T[t]$ also has an exponential tail. A simple generalization for $Z[t]$ in Eq. [1.7a]-[1.7d] would be either:

$$Z_E[t] \equiv +[G_o \, / \, (1 + \gamma_o \, t)] \, [\exp(-\delta_o t - q_o t^2)] \, , \qquad [2.6a]$$

$$Z_A[t] \equiv +[G_o \, / \, (1 + \gamma_o \, t)] \, [\exp(-\delta_o t)] = Z_E[t; \, q_o \equiv 0] \, . \qquad [2.6b]$$

As with Eq. [1.3c], the original CoVID-19 exponential growth factor K_A remains only as part of the G_o scaling factor, while the $\{\delta_o \to 0\}$ limit of Eq. [2.6b] converges back to the Eq. [1.3c] *Initial Model*.

Using Eq. [2.6a] for $Z_E[t]$ in the Eq. [2.2] $N(Z_E)$ example gives:

$$\rho[t] = \{dN[t] \, / \, dt\} = g_0 \, \tfrac{d}{dt} \exp[-Z_E] \, = -g_0 \, \exp[-Z_E] \, \tfrac{d}{dt} Z[t_E] = \qquad [2.7]$$
$$+N(Z_E) \, [\exp(-\delta_o t - q_o t^2)] \, \{ \tfrac{+G_o \, \gamma_o}{(1+\gamma_o \, t)^2} \, + \tfrac{G_o}{(1+\gamma_o \, t)} [+\delta_o + 2 q_o t] \} \, ,$$

which exhibits the following variety of long-time limits:

$$\rho[t; \, \delta_o = 0, \, q_o = 0] \to N(Z_E) \, \{ \tfrac{+G_o \, \gamma_o}{(1+\gamma_o \, t)^2} \} \, , \qquad [2.8a]$$

$$\rho[t; \; q_o = 0] \to N(Z_E) \, [\exp(-\delta_o t)] \, \{ \tfrac{+G_o \, \delta_o}{(1+\gamma_o \, t)} \} \, , \qquad [2.8b]$$

$$\rho[t; \; \delta_o = 0] \to N(Z_E) \, [\exp(-q_o t^2)] \, \{ \tfrac{2 \, G_o \, q_o}{\gamma_o} \} \, , \qquad [2.8c]$$

$$\rho[t] \to N(Z_E) \, \{\exp[-q_o (t + \tfrac{\delta_o}{2 q_o})^2]\} \, \{ \tfrac{2 \, G_o \, q_o}{\gamma_o} \exp[+\tfrac{1}{4} \delta_o^2 \, / \, q_o] \} \, . \qquad [2.8d]$$

Here, any $q_o \neq 0$ Gaussian component in $Z_E[t]$ gives a $\rho[t]$ tail that is also a pure Gaussian. An exponential component ($q_o \equiv 0$) in $Z_E[t]$ gives a time-modified exponential $\rho[t]$ tail, while having $\{q \equiv 0, \delta_o \equiv 0\}$ in $Z_E[t]$ gives the prior $\rho[t]\tilde{} \, (1 \, / \, t^2)$ result of Eq. [1.6b].

3 Pandemic Fast vs Slow Shutoffs

Each $Z_E[t]$ function modifies $N[t]$ predictions for the pandemic start, pandemic end, and the mid-range where $\rho[t]$ has its pandemic peak. The Eq. [2.6a] $Z_E[t]$ function especially alters the calculated CoVID-19 pandemic tail. For either $q_o \neq 0$ or $\delta_o \neq 0$, Eqs. [2.6a]-[2.6b] gives a pandemic *Fast Shutoff*, compared to the gradually decreasing $Z_o[t]$ of Eq. [1.3c] in the *Initial Model*, which is a pandemic *Slow Shutoff*. However $Z_o[t]$ from the *Initial Model*, and $Z_A[t]$ from Eq. [2.6b] both gave long-term $\rho[t]$ tails that decay much slower than the $q_o \neq 0$ Eq. [2.6a] Gaussian.

If data does not show evidence of a Gaussian pandemic *Fast Shutoff*, assuming the post-peak $\rho[t]$ data will be Gaussian is likely to provide optimistically inaccurate $N[t]$ predictions for CoVID-19 pandemic evolution. Apparently, this is exactly what was done by the *University of Washington IHME (Institute of Health Metrics and Evaluation)* in their widely publicized initial preprint[3] of 27 March 2020, with this Gaussian model continuing throughout their subsequent updates[4−6] up through 29 April 2020.

IHME changed everything in their 4 May 2020[7−8] update. They no longer used $\rho[t]$ Gaussian tails, and it doubled or tripled their predicted CoVID-19 pandemic death rates. Thus, unless the post-peak $\rho[t]$ exhibits Gaussian behavior, the $Z_A[t]$ with $\delta_o \neq 0$ is likely the most important modification to $Z_o[t]$, which is the pandemic *Fast Shutoff* model used here.

Using $Z_A[t]$, the pandemic *Fast Shutoff* can be extrapolated to calculate a pandemic start point where $N[t=0] = \mathbf{1}$. We then examine if this $Z_A[t]$ must also carry over to the $\rho[t]$ long-term tail,

Since the long-term low $\rho_{data}[t]$ tail may differ among localities, and is not well known, the $\delta_o \neq 0$ case of Eq. [2.6b] could end with a *Slow Shutoff*, giving:

$$Z_B[t] = +[G_o \,/\, (1+\gamma_o\, t)]\,\{\exp[-\delta_o t \,/\, (1+\lambda_o\, t)]\}\,, \qquad [3.1a]$$

$$\lim_{t\to\infty}\{Z_B[t]\} \approx +[G_o \,/\, (1+\gamma_o\, t)]\,\{\exp[-\delta_o \,/\, \lambda_o\,]\}\,, \qquad [3.1b]$$

with G_o as in Eq. [2.1a]. This Eq. [3.1a] $Z_B[t]$ function has the $\{\delta_o, \lambda_o\}$ *Mitigation Measure* operating at the start of *Social Distancing*, but reverting to the *Initial Model* in the long-time limit. Combining Eq. [2.6b] and Eq. [3.1a] cases gives this *Enhanced Initial Model (EIM)* equation:

$$Z_B[t] = +[G_o \,/\, (1+\gamma_o\, t)]\,\{\exp[-\delta_o t \,/\, (1+\kappa\gamma_o\, t)]\}\,, \qquad [3.2]$$

where $\kappa = 0$ is a pure exponential, and $\kappa = 1$ has a modified tail that includes its own long-term shutoff. Comparing $\kappa = \{0, 1\}$ in Eq. [3.2] provides a simple test for which model matches CoVID-19 data better in any locality. Any other $\kappa > 0$ value then recovers the more general $\lambda_o \equiv \kappa\gamma_o$ case. This Eq. [3.2] $Z_B[t]$ replaces $Z_o[t]$ of Eq. [1.3c], and its *EIM* companion $N_B[t]$ is:

$$N_B[t] = [e^{+G_o}]\,[\exp(-Z_B[t])\,, \qquad [3.3]$$

while using $Z[t] \to Z_B[t]$ in Eqs. [1.7a]-[1.7d] gives an *Enhanced Orthogonal Function [EOF]* model.

4 Finding $\{K_A, \gamma_o, \delta_o\}$ for $Z_B[t]$ from Data

If $\delta_o = 0$, the prior Eqs. [1.4a]-[1.5b] for $\{K_A, \gamma_o, \delta_o = 0\}$ and $\{t_I,\, t_F\}$ can be used, with the initial best-fit $\{K_o, \alpha_S\}$ values determined by minimizing the *rms* error between Eq. [1.2] and the measured data on a *Logarithmic Y-axis*. Unfortunately, Eqs. [1.4a]-[1.5b] cannot be used when $\delta_o \neq 0$, although finding a good $\{K_A, \gamma_o, \delta_o\}$ starting point is still needed for the *EIM*:

$$Z_B[t] = +[G_o \,/\, (1+\gamma_o\, t)]\,\{\exp[-\delta_o t \,/\, (1+\kappa\,\gamma_o\, t)]\}\,, \qquad [4.1a]$$

prior to any *EOF* analysis. The $\kappa = 1$ case also has this special symmetry:

$$[+\delta_o t \,/\, (1+\gamma_o\, t)] = (\delta_o \,/\, \gamma_o)\,[1 - \tfrac{1}{(1+\gamma_o\, t)}]\,, \qquad [4.2a]$$

$$\exp[-\delta_o t \,/\, (1+\gamma_o\; t)] = e^{-(\delta_o \,/\, \gamma_o)}\; \exp[+(\delta_o \,/\, \gamma_o)\tfrac{1}{(1+\gamma_o\, t)}]\,, \qquad [4.2b]$$

$$Z_B[t] = +[\tfrac{G_o}{(1+\gamma_o\, t)}]\, e^{-(\delta_o\,/\,\gamma_o)}\, \exp[+(\delta_o\,/\,\gamma_o)\tfrac{1}{(1+\gamma_o\, t)}]\,, \quad [4.2c]$$

$$Z_B[t] = +G_o\, [\tfrac{(\delta_o\,/\,\gamma_o)}{(1+\gamma_o\, t)}]\, \tfrac{1}{(\delta_o\,/\,\gamma_o)\, e^{+(\delta_o\,/\,\gamma_o)}}\, \exp[+(\delta_o\,/\,\gamma_o)\tfrac{1}{(1+\gamma_o\, t)}]\,, \quad [4.2d]$$

which can re-written as:

$$W(X[t]) \equiv X[t]\, \exp(+X[t])\,, \quad [4.3a]$$

$$X[t] = [(\delta_o\,/\,\gamma_o)\,/\,(1+\gamma_o\, t)]\,, \quad [4.3b]$$

$$X[0] = [\delta_o\,/\,\gamma_o]\,, \quad [4.3c]$$

$$Z_B[t]_{\kappa=1} = +G_o\; W(X[t])\,/\,W(X[0])\,. \quad [4.3d]$$

$$N_B(Z_B) = [e^{+G_o}]\, \exp(-Z_B[t]_{\kappa=1})\,, \quad [4.3e]$$

while the $\kappa = 0$ case is:

$$Z_A[t] = +[G_o\,/\,(1+\gamma_o\, t)]\, \exp(-\delta_o t)\,, \quad [4.4a]$$

$$N_A(Z_A) = [e^{+G_o}]\, \exp(-Z_B[t]_{\kappa=0}) = [e^{+G_o}]\, \exp(-Z_A[t]). \quad [4.4b]$$

For $\kappa = \{0, 1\}$, the $t = 0$ point, G_o from Eq. [2.1a], and the $N_I(t_I)$ and $N_F(t_F)$ initial and final points, give these equations to help set $\{K_A, \gamma_o, \delta_o\}$:

$$N_I[t=0] = \mathbf{1} = G_o\, \exp(-Z_B[t=0])\,, \quad [4.5a]$$

$$N_I[t_I] = N_I = G_o\, \exp(-Z_B[t_I])\,, \quad [4.5b]$$

$$N_F[t_F] = N_F = G_o\, \exp(-Z_B[t_F])\,, \quad [4.5c]$$

for the *EIM*. Minimizing the *rms* error between the Eq. [3.3] $\{K_A, \gamma_o, \delta_o, t_I\}$ functions and measured data on a *Logarithmic Y-axis* can be done as follows. Start with estimated values for $\{\widehat{K}_A, \widehat{\gamma}_o, \widehat{\delta}_o, \widehat{t}_{offset}\}$ in:

$$\widehat{Z}[t] = +[\widehat{G}_o\,/\,(1+\widehat{\gamma}_o\, t)]\, \{\exp[-\widehat{\delta}_o t\,/\,(1+\kappa\,\widehat{\gamma}_o\, t)]\}\,, \quad [4.6a]$$

$$\widehat{N}[t] = [e^{+\widehat{G}_o}]\, [\exp(-\widehat{Z}[t])\,, \quad [4.6b]$$

$$\widehat{G}_o \equiv (\widehat{K}_A\,/\,\widehat{\gamma}_o)\,, \quad [4.6c]$$

$$t = (t_{data} - \widehat{t}_{offset})\,, \quad [4.6d]$$

where t_{data} is the data start time. Set a preliminary value for $\widehat{t}_{offset}$ first, to fix the time scale for the $N_{data}[t]$ measured values:

$$N_I \equiv N_{data}[t^I_{data} - \widehat{t}_{offset}]\,, \quad [4.7a]$$

$$N_F \equiv N_{data}[t^F_{data} - \widehat{t}_{offset}]\,, \quad [4.7b]$$

$$(t_F - t_I) \equiv (t^F_{data} - t^I_{data})\,. \quad [4.7c]$$

Next, pick values for $\{\widehat{\gamma}_o, \widehat{\delta}_o\}$ for $\widehat{N}[t]$ in Eq. [4.6b], allowing direct comparison between $N[t]$ and $\widehat{N}[t]$ at each data point:

$$\widehat{N}[t] \equiv \widehat{N}[t = (t_{data} - \widehat{t}_{offset})]\,, \quad [4.8a]$$

$$N_{data}[t] \equiv N_{data}[t = (t_{data} - \widehat{t}_{offset})]\,. \quad [4.8b]$$

The resulting calculated values for both $\{\widehat{N}[t_I],\, \widehat{N}[t_F]\}$ can often be much too high or low, compared to the $\{N_I,\, N_F\}$ measured data, but those values can be renormalized to:

$$\overline{N}[t] = \widehat{N}[t]\; (N_I\,/\,\widehat{N}[t_I]) \equiv S_I\, \widehat{N}[t]\,, \quad [4.9a]$$

$$\overline{N}[t_F] = \widehat{N}[t_F]\; (N_I\,/\,\widehat{N}[t_I]) \equiv S_I\, \widehat{N}[t_F]\,. \quad [4.9b]$$

Here, S_I is the renormalization coefficient, and $\overline{N}[t]$ allows easy comparison to the measured $N_{data}[t]$ since $\overline{N}[t_I] \equiv N_I$. Given $\{\widehat{\gamma}_o, \widehat{\delta}_o\}$, the $\widehat{K}_A(\widehat{\gamma}_o)$ value that is needed to obey $\overline{N}[t_F] \rightarrow N_F$ can be set by using *Excel*^{TM}_*Goal-Seek* or its equivalent, which also sets a particular S_I value. Next, the $\widehat{\gamma}_o$ value is adjusted to find the specific $\{K_A,\, \gamma_o\}$ parameter pair that gives $S_I = 1$. This process is needed because these $\widehat{\delta}_o \neq 0$ cases do not allow easy determination of t_I as in Eq. [1.4a], or for $\{K_A,\, \gamma_o\}$, given t_I, as in Eqs. [1.5a]-[1.5b].

The *rms* error on a *Logarithmic Y-axis*, between this $\overline{N}[t\,;\,K_A,\,\gamma_o]$ and the $N_{data}[t]$ is one of many $\{K_A,\,\gamma_o,\widehat{\delta}_o,\widehat{t}_{offset};\,S_I=1\}$ choices. The minimum *rms* error among all these $S_I=1$ cases and the $N_{data}[t]$, when varying $\{\widehat{\delta}_o,\,\widehat{t}_{offset}\}$ gives the best $\{K_A,\gamma_o,\delta_o,t_{offset}\}$ values for Eqs. [4.3a]-[4.3e].

5 *Enhanced Initial Model [EIM]* Results for Italy

The Eq.[1.3a] *Initial Model* results were shown in **Figs. 1-2**. Mandatory *Social Distancing* was introduced at $N_{data}^{3/10/2020}=10,149$ which is the t_I data point, with $N_{data}^{6/15/2020}=237,290$ being the t_F data point. The *EIM* was then applied to the same data, to highlight the improvements that can be obtained from using the *EIM* of $Z_A[t]$ and $N_A(Z_A)$, in place of $Z_o[t]$ and $N_o(Z_o)$.

Figures 3-4 show the resulting *EIM* best-fits for $Z_A[t]$ and $N_A(Z_A)$, along with using a $\rho_A[t]$ tail that is a pure exponential decay.

For the *EIM*, a new best estimate of $t_{offset}=2.866\,days$ was found within the $N_{data}^{2/23/2020}$ $(Day\ 1)$ to $N_{data}^{3/10/2020}$ $(Day\ 17)$ data, setting the *EIM* $t=0$ point. Then $t_I=(17-2.866)=14.134\,days$, while $N_{data}^{6/15/2020}$ $(Day\ 114)$ gives $t_F=(114-2.866)\ =111.134\,days$, along with:

$$N_{data}^{3/10/2020}[t_I=14.134]=10,149\,; \tag{5.1a}$$
$$N_{data}^{6/15/2020}[t_F=111.134]=237,290\,; \tag{5.1b}$$
$$N_{data}^{2/25/2020}[t=0]=\mathbf{1}\,, \tag{5.1c}$$
$$(t_F-t_I)=97\,days\,. \tag{5.1d}$$

This X-axis $t=0$ point is a hypothetical *EIM* pandemic starting point, if *Social Distancing* had been operating throughout the initial CoVID-19 period. **Figure 3** has a predicted CoVID-19 pandemic peak of $\tilde{}5,217\,/\,day$ at $t=29.134\,days$ on 3/25/2020, with $\tilde{}243,100$ total cases at the pandemic end. This datafit has $>4X$ error reduction over the $\delta_o=0$ case, as summarized next:

K_A	γ_o	$t_{dbl},days$	$N[t\rightarrow\infty]$	δ_o	$t_I\,,days$	rms_{ERR}
1.285 436	.101062	.553060	$\tilde{}243,100$	.0336	14.134	0.023755
4.240513	.33078	.163458	$\tilde{}338,165$	**0**	7.899	0.097828

[5.2]

The *EIM* with $Z_A[t]$ and $\delta_o=0.0336$ gives a $\rho_A[t]$ curve that is in excellent agreement with the **Fig. 3** measured $\rho_{data}[t]$ data. Comparing $N_A[t]$ and $N_{data}[t]$ in **Fig. 4** also shows an excellent match over the whole *Logarithmic Y-axis* range, used in the *rms* error minimization.

The **Figs. 3-4** $\kappa=0$ results were then compared to the $\kappa=1$ case, using $Z_B[t]$ and $N_B(Z_B)$ of Eqs. [3.2]-[3.3]. The $\kappa=1$ case has a *Social Distancing* factor that gradually turns off the *EIM* exponential decay. The resulting *rms* error best fits converged to $\delta_o\rightarrow 0$, as follows:

γ_o	t_{dbl}	rms_{ERR}	δ_o	t_{offset}^{days}	$t_I^{days}::t_F^{days}$
.07146	.775863	.2223783	.2000	10.0	7 :: 104
.18623	.295372	.1751635	.2000	11.0	6 :: 103
.30360	.181417	.2102839	.2000	12.0	5 :: 102

.39748	.137925	.1430275	.0500	11.0	6 :: 103
.43604	.125722	.1425737	.0135	11.0	6 :: 103
.44265	.123844	.1425524	.0070	11.0	6 :: 103
.44466	.123284	.1425480	.0050	11.0	6 :: 103
.44868	.122179	.1425445	.0010	11.0	6 :: 103
.44968	.121907	.1425442	.0000	11.0	6 :: 103 . [5.3]

This $\kappa = 1$ result shows that the process giving rise to exponential tails in the $\rho_{data}[t]$ for a pandemic *Fast Shutoff* is independent of the *Social Distancing* process that gradually lengthens the t_{dbl} *doubling time*, as measured by γ_o. Comparing the $\kappa = \{0, 1\}$ cases shows that the pure exponential tail with $Z_A[t] = Z_B[t]_{\kappa=0}$ matches the $\rho_{data}[t]$ data best.

6 *Enhanced Orthogonal Functions* for Italy

Any monotonic $Z[t]$ can convert measured $N_{data}[t]$ data into $N_{data}(Z)$. Using the Eq. [2.6b] $Z_A[t] \to Z[t]$ in Eqs. [1.7a]-[1.7d] extends the *EIM* into an *EOF* model, where Eq. [1.9] gives:

$$\rho[t] = R(Z_A[t])\,\tfrac{dZ_A}{dt} = Z_A[t]\,R(Z_A[t])\,\{\delta_o + \tfrac{\gamma_o}{(1+\gamma_o\,t)}\}\,, \quad [6.1a]$$

$$Z_A[t] = +[G_o\,/\,(1+\gamma_o\,t)]\,\exp(-\delta_o t)\,. \quad [6.1b]$$

The Eq. [5.2] $\delta_o \neq 0$ entries and Eq. [5.1a]-[5.1d] boundary conditions give:

$$Z_A^{\min}[t_F = 111.134] = 0.024226510\,, \quad [6.2a]$$

$$Z_A^{\max}[t_I = 14.134] = 3.176125728\,. \quad [6.2b]$$

These data-driven $Z_A[t]$ limits are used next, along with $Z[t] \to Z_A[t]$ in:

$$N(Z) = \sum_{m=0}^{m=M_F} g_m\,L_m(Z)\,\exp[-Z]\,, \quad [6.3a]$$

$$g_n \equiv \sum_{m=0}^{m=M_F} g_m \int_{Z=0}^{Z=+\infty} L_n(Z)\,L_m(Z)\,\exp[-Z]\,dZ = \quad [6.3b]$$

$$\int_{Z=Z_A^{\min}}^{Z=Z_A^{\max}} L_n(Z)N_{data}(Z)dZ +$$

$$\int_{Z=Z_A^{\max}}^{Z=+\infty} L_n(Z)N(Z)dZ + \int_{Z=0}^{Z=Z_A^{\min}} L_n(Z)N(Z)dZ\,,$$

where $m = \{0, M_F\}$ sets how many terms are in the Eq. [6.3a] series. Generally $M_F = 2$ is used here. The $L_m(Z)$ are the *Laguerre Polynomials*, with the first few $L_m(Z)$ being:

$$L_{-1}(Z) \equiv 0\,, \quad [6.4a]$$

$$L_0(Z) \equiv 1 = L_m(Z=0)\,, \quad [6.4b]$$

$$L_1(Z) \equiv (1 - Z)\,, \quad [6.4c]$$

$$L_2(Z) \equiv (1 - 2\,Z + \tfrac{1}{2}Z^2)\,, \quad [6.4d]$$

$$L_3(Z) \equiv (1 - 3\,Z + \tfrac{3}{2}Z^2 - \tfrac{1}{6}Z^3)\,, \quad [6.4e]$$

$$L_4(Z) \equiv (1 - 4\,Z + 3\,Z^2 - \tfrac{2}{3}Z^3 + \tfrac{1}{24}Z^4)\,. \quad [6.4f]$$

Some important properties of the *Laguerre Polynomials* are:

$$\int_{Z=0}^{Z=+\infty} L_m(Z)\,L_n(Z)\,\exp(-Z)\,dZ = \mathbf{1}\,\delta_{m,n}\,, \quad [6.5a]$$

$$\delta_{m,n} = \begin{pmatrix} \mathbf{1} & for\ m{=}n \\ \mathbf{0} & otherwise \end{pmatrix}, \qquad [6.5b]$$

$$\int_{Z'=Z}^{Z'=+\infty} L_m(Z')\,\exp(-Z')\,dZ' = [L_m(Z) - L_{m-1}(Z)]\,\exp(-Z)\,, \qquad [6.5c]$$

$$L_m(Z)\,\exp(-Z) = \tfrac{1}{m!}\tfrac{d^m}{dZ^m}[Z^m\,e^{-Z}] = e^{-Z}\sum_{k=0}^{k=m}(-1)^k\tfrac{m!}{k!\,(m-k)!}\left[\tfrac{Z^k}{k!}\right], \qquad [6.5d]$$

$$L_{m\geq 2}(Z) = [2 - \tfrac{(Z+1)}{m}]\,L_{m-1}(Z) - [1 - \tfrac{1}{m}]\,L_{m-2}(Z)\,. \qquad [6.5e]$$

Here Eq. [6.5a] defines an *orthogonal function set*. The "**n!**" (**n**-*factorial*) in Eq. [6.5d], for **n** an integer, is defined as the product:

$$\mathbf{n}! \equiv (\mathbf{n})(\mathbf{n}-1)(\mathbf{n}-2)(\mathbf{n}-3)...(3)(2)(1)\,, \qquad [6.6a]$$

$$\mathbf{1}! \equiv \mathbf{0}! \equiv 1\,, \qquad [6.6b]$$

where *factorials* with negative integers are not allowed. For $M_F > 2$, the following equations developed by Watson[10], and improved by Gillis and Weiss[11], helps in evaluating Eq. [6.3b]:

$$L_r(Z)\,L_s(Z) = \sum_{t=|r-s|}^{t=(r+s)} C_{rst}\;L_t(Z)\,, \qquad [6.7a]$$

$$C_{rst} = \int_{X=0}^{X=+\infty} L_r(X)\,L_s(X)\,L_t(X)\,\exp(-X)\;dX\,, \qquad [6.7b]$$

$$C_{rst} \equiv \tfrac{(-1)^p}{2^p}\sum_{n=0}^{n=(r+s)}(2^{2n})\tfrac{(r+s-n)!}{(r-n)!\,(s-n)!\,(2n-p)!\,(p-n)!}, \qquad [6.7c]$$

$$p \equiv (r+s-t), \qquad [6.7d]$$

where ALL terms in the Eq. [6.7c] sum for $n = \{0, (r+s)\}$ have an implicit requirement that all negative *factorial* arguments are excluded[10–11].

Since the $N(Z)$ of Eq. [6.3a] has $\{g_m;\ m = (0, M_F)\}$, and $N(Z)$ also appears in each g_n-equation of Eq. [6.3b], how to determine each g_m by itself, can be done as follows. First define:

$$Q_n \equiv \int_{Z=Z_A^{\min}}^{Z=Z_A^{\max}} L_n(Z)\,N_{data}(Z)\,dZ\,, \qquad [6.8a]$$

$$K_{m,n} \equiv \int_{Z=Z_A^{\min}}^{Z=Z_A^{\max}} L_m(Z)\,L_n(Z)\,\exp(-Z)\,dZ = K_{n,m}\,. \qquad [6.8b]$$

When the $N_{data}(Z)$ is comprised of $j = \{1, 2, ...J\}$ discrete values between $\{Z_A^{\min},\ Z_A^{\max}\}$, with each Z_j having an $N_{data}^{(j)}(Z_j)$ value, the Eq. [6.8a] integral needs to be replaced by a sum. Let $Z_0 = Z_1$ and $Z_{J+1} = Z_J$, the Q_n replacement for Eq. [6.8a] is then:

$$Q_n \equiv \sum_{j=1}^{j=J} L_n(Z_j)\;N_{data}^{(j)}(Z_j)\;\Delta_j\,, \qquad [6.9a]$$

$$\Delta_j \equiv \tfrac{1}{2}|Z_{j+1} - Z_{j-1}|\,. \qquad [6.9b]$$

Eq. [6.3b] can then be re-written as a 3×3 matrix $\underline{\mathbf{M}}_3$, which relates a data-driven $\overrightarrow{Q}_3$-vector to a resultant $\overrightarrow{g}_3$-vector:

$$\overrightarrow{Q}_3 \;=\; \underline{\mathbf{M}}_3\;\overrightarrow{g}_3\,, \qquad [6.10a]$$

$$\begin{pmatrix} Q_o \\ Q_1 \\ Q_2 \end{pmatrix} = \begin{pmatrix} K_{0,0} & K_{0,1} & K_{0,2} \\ K_{1,0} & K_{1,1} & K_{1,2} \\ K_{2,0} & K_{2,2} & K_{2,2} \end{pmatrix} \begin{pmatrix} g_0 \\ g_1 \\ g_2 \end{pmatrix}. \qquad [6.10b]$$

$$(\underline{\mathbf{M}}_3)^{-1}\ \overrightarrow{Q}_3\ \equiv \overrightarrow{g}_3\,, \qquad [6.10c]$$

where $(\underline{\mathbf{M}}_3)^{-1}$ is the matrix inverse of $\underline{\mathbf{M}}_3$. When $\{Z_A^{\min},\ Z_A^{\max}\} \to \{0, +\infty\}$, this $\underline{\mathbf{M}}_3$ becomes the Identity Matrix. The following $k_{m,n}(Z)$ integrals set $K_{m,n}$:

$$k_{m,n}(Z) = \int_{Z'=Z}^{Z'=+\infty} L_m(Z')\, L_n(Z')\, \exp(-Z')\, dZ' = k_{n,m}(Z)\,, \qquad [6.11a]$$

$$K_{m,n} \equiv k_{m,n}(Z_A^{\min}) - k_{m,n}(Z_A^{\max}) = K_{n,m}\,. \qquad [6.11b]$$

The $k_{m,n}(Z)$ integrals can be determined using Eq. [6.5c], which gives:

$$k_{0,0}(Z) = 1\exp(-Z)\,, \qquad [6.12a]$$

$$k_{1,1}(Z) = \{1\ + Z^2\}\exp(-Z)\,, \qquad [6.12b]$$

$$k_{2,2}(Z) = \{1 + 2\,Z^2 - Z^3 + \tfrac{1}{4}Z^4\}\exp(-Z)\,, \qquad [6.12c]$$

$$k_{0,1}(Z) = (-Z)\ \exp(-Z)\,, \qquad [6.12d]$$

$$k_{0,2}(Z) = (-Z)\,\{1 - \tfrac{1}{2}Z\}\exp(-Z)\,, \qquad [6.12e]$$

$$k_{1,2}(Z) = (-Z)\,\{1 - Z + \tfrac{1}{2}Z^2\}\exp(-Z)\,. \qquad [6.12f]$$

To extract $\{g_0,\, g_1,\, g_2\}$, the 3×3 symmetric $\underline{\mathbf{M}}_3$ matrix needs inversion:

$$\underline{\mathbf{M}} = \begin{pmatrix} a & d & f \\ d & b & e \\ f & e & c \end{pmatrix}\,, \qquad [6.13a]$$

$$\det[\underline{\mathbf{M}}] \equiv [abc - ae^2 - bf^2 - cd^2 + 2\,def]\,, \qquad [6.13b]$$

$$\det[\underline{\mathbf{M}}]\ (\underline{\mathbf{M}})^{-1}\ \equiv \begin{pmatrix} [bc - e^2] & -(cd - ef) & -(bf - de) \\ -(cd - ef) & [ac - f^2] & -(ae - df) \\ -(bf - de) & -(ae - df) & [ab - d^2] \end{pmatrix}\,, \qquad [6.13c]$$

which determines $\{g_0,\, g_1,\, g_2\}$ from the $\{Q_0,\, Q_1,\, Q_2\}$ data. A best-fit $N(Z)$ for $Z = \{0^+, \infty^-\}$ results, along with an equivalent fit for $R(Z)$ using Eq. [1.7d].

Instead of having to find the best $\{g_0,\, g_1,\, g_2\}$ triplet, one could find the best $\{g'_0,\, g'_1\}$ by just using using $\{Q_0,\, Q_1\}$ and an $\underline{\mathbf{M}}_2$ sub-matrix; or one could find the best $\{g_0^+\}$ by itself by just using $\{Q_0\}$ and an $\underline{\mathbf{M}}_1$ sub-matrix:

$$\overrightarrow{Q}_2\ =\ \underline{\mathbf{M}}_2\ \overrightarrow{g}_2\,, \qquad [6.14a]$$

$$\begin{pmatrix} Q_o \\ Q_1 \end{pmatrix} = \begin{pmatrix} K_{0,0} & K_{0,1} \\ K_{1,0} & K_{1,1} \end{pmatrix} \begin{pmatrix} g'_0 \\ g'_1 \end{pmatrix}\,, \qquad [6.14b]$$

$$\begin{pmatrix} g'_0 \\ g'_1 \end{pmatrix} = \begin{pmatrix} K_{0,0} & K_{0,1} \\ K_{1,0} & K_{1,1} \end{pmatrix}^{-1} \begin{pmatrix} Q_o \\ Q_1 \end{pmatrix} = \frac{1}{[K_{0,0}\,K_{1,1} - K_{0,1}\,K_{1,0}]} \begin{pmatrix} K_{1,1} & K_{1,0} \\ K_{0,1} & K_{0,0} \end{pmatrix} \begin{pmatrix} Q_o \\ Q_1 \end{pmatrix}, \qquad [6.14c]$$

$$\overrightarrow{Q}_1\ =\ \underline{\mathbf{M}}_1\ \overrightarrow{g}_1\,, \qquad [6.14d]$$

$$\begin{pmatrix} Q_o \end{pmatrix} = \begin{pmatrix} K_{0,0} \end{pmatrix} \begin{pmatrix} g_o^+ \end{pmatrix}\,, \qquad [6.14e]$$

$$\begin{pmatrix} g_o^+ \end{pmatrix} = \begin{pmatrix} K_{0,0} \end{pmatrix}^{-1} \begin{pmatrix} Q_o \end{pmatrix}\,. \qquad [6.14f]$$

Once the $\{g_m;\ m = (0, M_F)\}$ constants are found and used in Eq. [1.8], its c_0 value provides the new *EOF* estimate for the predicted total number of CoVID-19 cases at the pandemic end, refining the initial Eq. [5.2] $N[t \to \infty]$ *EIM* value.

7 *EOF* Model Results for Italy

The *EOF* model starts with the *EIM* of Eq. [2.6b] using $Z_A[t]$, and the *bing.com* Italy data[9], which gives:

$$N_{data}[t_I = 14.134] = 10,149\,; \quad [7.1a]$$
$$N_{data}[t_F = 111.134] = 237,290\,; \quad [7.1b]$$
$$N_A[t \to \infty] = 243,109\,, \quad [7.1c]$$
$$Z_A^{\min}[t_F = 111.134] = 0.024226510\,, \quad [7.1d]$$
$$Z_A^{\max}[t_I = 14.134] = 3.176125728\,, \quad [7.1e]$$

via Eqs. [5.1a]-[5.1d], [5.2], and [6.2a]-[6.2b]. For these $\{Z_A^{\min},\, Z_A^{\max}\}$ values, with $(t_F - t_I) = 97\ days$, the $\underline{\mathbf{M}}_3$ matrix of $K_{m,n}$ entries, via Eq. [6.8b], is:

$$\underline{\mathbf{M}}_3 = \begin{pmatrix} K_{0,0} & K_{0,1} & K_{0,2} \\ K_{1,0} & K_{1,1} & K_{1,2} \\ K_{2,0} & K_{2,2} & K_{2,2} \end{pmatrix} = \begin{pmatrix} 0.93432 & 0.10895 & -0.10133 \\ 0.10895 & 0.51376 & 0.35717 \\ -0.10133 & 0.35717 & 0.36868 \end{pmatrix} \quad [7.2]$$

It has a rather small $\det[\underline{\mathbf{M}}_3] = 0.04024218$ value, with an inverse of:

$$(\underline{\mathbf{M}}_3)^{-\mathbf{1}} \equiv \begin{pmatrix} 1.536\,745 & -1.897\,502 & 2.260\,643 \\ -1.897\,502 & 8.304\,570 & -8.566\,823 \\ 2.260\,643 & -8.566\,823 & 11.633\,092 \end{pmatrix}. \quad [7.3]$$

A convolution of $L_m(Z_A)$ functions with the measured $\overrightarrow{Q}_3$ dataset vector of Eqs. [6.9a]-[6.9b], along with the above $(\underline{\mathbf{M}}_3)^{-\mathbf{1}}$, gives this final $\overrightarrow{g}-$vector[12]:

$$(\underline{\mathbf{M}}_3)^{-\mathbf{1}}\ \overrightarrow{Q}_3 \equiv (\underline{\mathbf{M}}_3)^{-\mathbf{1}} \begin{pmatrix} Q_o \\ Q_1 \\ Q_2 \end{pmatrix} = (\underline{\mathbf{M}}_3)^{-\mathbf{1}} \begin{pmatrix} +226,767 \\ +26,978 \\ -22,399 \end{pmatrix} \equiv$$

$$\overrightarrow{g}_3 = \begin{pmatrix} g_o \\ g_1 \\ g_2 \end{pmatrix} = \begin{pmatrix} +246,656 \\ -14,362 \\ +20,954 \end{pmatrix}, \quad [7.4]$$

determining the constants for $N(Z_A)$ in Eq. [1.7a]. The coefficients for $R(Z_A)$, which sets the predicted number of daily new CoVID-19 cases, are:

$$\overrightarrow{C}_3 = \begin{pmatrix} 1 & 1 & 1 \\ 0 & 1 & 1 \\ 0 & 0 & 1 \end{pmatrix} \overrightarrow{g}_3 = \begin{pmatrix} c_0 \\ c_1 \\ c_2 \end{pmatrix} = \begin{pmatrix} +253,248 \\ +6,592 \\ +20,954 \end{pmatrix}, \quad [7.5]$$

determining the constants needed for $R(Z_A)$ in Eq. [1.7b]. Using these $\{g_0,\, g_1,\, g_2\}$ values along with Eq. [1.8] gives:

$$N(Z_A \to 0) \equiv N[t \to \infty] = c_0 \equiv \{253,248\}\,, \quad [7.6]$$

as a new predicted total number of CoVID-19 cases at the pandemic end for the *EOF* model, which is a ˜4.17% or 10,139 increase in the number of cases, compared to the *EIM* value of Eq. [7.1c].

Using Eq. [6.1b] for $Z_A[t]$, and substituting the Eq. [7.3] $\overrightarrow{C}_3$ values into Eq. [1.7b] gives $R(Z_A)$. The $\rho[t]$ in Eq. [6.1a] is derived from $R(Z_A)$ using Eq. [1.7b], with the resulting *EOF* $\rho[t]$ plotted in **Figure 5**, along with the $t > t_I$ raw data for the daily new CoVID-19 cases.

The **Figure 5** *EOF* model also gives a $t < t_I$ extrapolation, which shows what the combination of processes would look like, if they all had been operating continuously from the CoVID-19 pandemic start. The companion $N[t]$ analytic

result, along with the $t > t_I$ raw data for the total number of CoVID-19 cases is show in **Figure 6**.

Comparing the size and timing of the $\rho[t]$ pandemic peak, and its Day 200 value, between the *EIM* (**Figs. 3-4**) and *EOF* model (**Figs. 5-6**), gives:

$$\begin{pmatrix} \text{Parameter} & \textit{EIM} & \textit{EOF Model} \\ N[t \to \infty] & 243,109 & 253,248 \\ \max\{\rho[t_p]\} & 5,217 \ / \ day & 5,142 \ / \ day \\ [t_p] \ Date & 3/25/2020 & 3/27/2020 \\ \overset{200}{Day} \rho[t] & 6.67 \ / \ day & 7.59 \ / \ day \end{pmatrix}, \qquad [7.7]$$

showing the *EOF* model predicts more cases total and more daily new CoVID-19 cases at Day 200, as well as modifying the pandemic peak predictions.

While the above analysis used $M_F = 2$, with the Eq. [7.4] $\overrightarrow{g}_3$ setting the best $\{g_0, g_1, g_2\}$ values, this *EOF* model also provides estimates for the simpler $M_F = \{0, 1\}$ cases, as outlined by Eqs. [6.14a]-[6.14f]. For $M_F = 1$, the best two $\{g_0', g_1'\}$ values were gotten by only using $\{Q_0, Q_1\}$ and an $\underline{\mathbf{M}}_2$ sub-matrix of $\underline{\mathbf{M}}_3$. For $M_F = 0$, the best $\{g_0^+\}$ by itself is derived by using $\{Q_0\}$ and the $\underline{\mathbf{M}}_1$ sub-matrix. These alternative estimates give:

$$\overrightarrow{g}_2 = \begin{pmatrix} g_0' \\ g_1' \end{pmatrix} = \begin{pmatrix} .93432 & .10895 \\ .10895 & .51376 \end{pmatrix}^{-1} \begin{pmatrix} 226,767 \\ 26,978 \end{pmatrix} = \begin{pmatrix} 242,584 \\ 1,069 \end{pmatrix}$$

$$\overrightarrow{g}_1 = \begin{pmatrix} g_0^+ \end{pmatrix} = \begin{pmatrix} 0.93432 \end{pmatrix}^{-1} \begin{pmatrix} +226,767 \end{pmatrix} = \begin{pmatrix} 242,709 \end{pmatrix}. \qquad [7.8a]\text{-}[7.8b]$$

These additional calculations give the following progression of estimates for $N[t \to \infty]$, which is the final number of CoVID-19 cases at the pandemic end:

$$\begin{pmatrix} N_A[t \to \infty; \ EIM \,] \\ g_o^+ \\ c_o' = g_0' + g_1' \\ c_o = g_0 + g_1 + g_2 \end{pmatrix} = \begin{pmatrix} 243,109 \\ 242,709 \\ 243,653 \\ 253,248 \end{pmatrix}, \qquad [7.9]$$

based on increasing the number of data fitting parameters used with the original data. This summary shows the $N[t \to \infty]$ projections are fairly stable, with an average and 1σ standard deviation:

$$< N[t \to \infty] > = \ 245,680 \ \pm \ 5,060 \,; \qquad [7.10]$$

among these different calculations, where 1σ is ˜2.06% of the overall average.

Comparing the results among **Figs. 1-6** also highlights these items:

(a) All $\rho[t]$ functions have a sharp rise, and slower decreasing tail. The fastest changing $\rho_{data}[t]$ tail, as in the Italy CoVID-19 (*Fast Shutoff*) data, was successfully modeled by adding in an exponential term, as in Eq. [6.1b].

(b) The datafits in **Fig. 4** and **Fig. 6** show that the extra parameters in the *EIM* and *EOF* model fits the $\rho_{data}[t]$ shape progressively better.

(c) The *EOF* model shows only relatively small changes of ˜2.06% in the $N[t \to \infty]$ limits (Eq. [7.10]), as an estimate of uncertainty in the *EIM*.

(d) The *Enhanced Initial Model (EIM)* function captures much of the progression to a pandemic *Fast Shutoff*, as seen in the Italy data.

The $\rho[t]$ tail may still differ from these predictions, due to factors such as:

(i) The CoVID-19 dynamics may change in the long-term low $\rho[t]$ regime;

(ii) A "second wave" or multiple waves of $\rho[t]$ resurgence may occur, which are beyond the scope of this CoVID-19 pandemic modeling.

8 Summary and Conclusions

The early stages of the CoVID-19 coronavirus pandemic starts off with a nearly exponential rise in the number of infections with time. Defining $N[t]$ as the expected total number of CoVID-19 cases vs time, this basic function:

$$N_o[t] = \mathbf{1}\exp[+K_A\,t\,/\,(1+\gamma_o\,t)] = \exp[+G_o]\,\exp[-Z_o]\,, \quad [8.1a]$$
$$Z_o[t] \equiv +[G_o\,/\,(1+\gamma_o\,t)]\,,\; G_o \equiv [K_A\,/\,\gamma_o]\,, \quad [8.1b]$$
$$\rho_o[t] \equiv dN_o[t]\,/\,dt\,, \quad [8.1c]$$

models *Social Distancing* effects as a gradual lengthening of the pandemic growth *doubling time*, which enables pandemic shutoff with only a small population of infected persons. The Eq. [8.1b] $Z_o[t]$ was our *Initial Model*[1], and gives a CoVID-19 *Slow Shutoff* with a long-term $\rho_o[t]\tilde{}[1/t^2]$ tail. Previously we showed[1–2] that this $Z_o[t]$ model fits many $N_{data}[t]$ and $\rho_{data}[t]$ cases.

However, some data had a CoVID-19 *Fast Shutoff*, with a $\rho_{data}[t] \sim [\exp(-\delta_o t)]$ exponential tail, such as in Italy[9], where a Gaussian tail $\rho[t] \sim [\exp(-q_o\,t^2)]$ would have decreased too quickly. An *Enhanced Initial Model (EIM)* was developed here, using this $Z_A[t]$ function:

$$N_A[t] \approx \mathbf{1}\exp[+G_o]\,\exp(-Z_A[t])\,, \quad [8.2a]$$
$$Z_A[t] \equiv +[G_o\,/\,(1+\gamma_o\,t)]\,\exp(-\delta_o t)\;, \quad [8.2b]$$
$$G_o \equiv [K_A\,/\,\gamma_o]\,, \quad [8.2c]$$
$$\rho_A[t] \equiv dN_A[t]\,/\,dt\,. \quad [8.2d]$$

We also examined if the $\exp(-\delta_o t)$ exponential decay could also be subject to a *Slow Shutoff*, giving $\exp[-\delta_o t\,/\,(1+\gamma_o\,t)]$ instead of $\exp(-\delta_o t)$, but that did not match the Italy data. To allow more data fitting parameters beyond just $\{K_A,\,\gamma_o,\,\delta_o\}$, an orthogonal function method was developed[2]:

$$N(Z) = \sum_{m=0}^{m=M_F} g_m\,L_m(Z)\,\exp[-Z]\,, \quad [8.3a]$$
$$R(Z) = \sum_{m=0}^{m=M_F} c_m\,L_m(Z)\,\exp[-Z]\,, \quad [8.3b]$$
$$N(Z) \equiv \int_{Z'=Z}^{Z'=+\infty} R(Z')\,d\,Z'\,, \quad [8.3c]$$
$$c_{M_F-k} = \sum_{m=0}^{m=k} g_m\,, \quad [8.3d]$$

which is applicable to a generic $Z[t]$ function, with $N[t] = N(Z[t])$, where $Z[t] \to Z_o[t]$ and $Z[t] \to Z_A[t]$ are special cases. Larger M_F with more $\{L_m(Z);\, m = (0, +M_F)\}$ terms can match almost any *arbitrary function*, enabling fits to a variety of $N[t]$ and $\rho[t]$ shapes. The $\{g_m;\, m = (0, +M_F)\}$ are constants determined from each dataset. The $L_m(Z)$ are the *Laguerre Polynomials*, with several important properties given in Eqs. [6.4a]-[6.5e].

Using $Z_A[t]$ in Eqs. [8.3a]-[8.3d] results in this *Enhanced Orthogonal Function [EOF]* model, which is applicable to both *Slow* or *Fast Shutoff* CoVID-19 pandemic data. The $\rho[t]$ expected number of daily new CoVID-19 cases is:

$$N[t] \equiv \int_{t'=(-1/\gamma_o)}^{t'=t} \rho[t']\,dt'\,, \quad [8.4a]$$

$$\rho[t] = R(Z_A[t])\,\frac{dZ_A}{dt} = R(Z_A[t])\,\left[\frac{G_o}{(1+\gamma_o\,t)}\right]\left\{\delta_o + \frac{\gamma_o}{(1+\gamma_o\,t)}\right\}\left[\exp(-\delta_o t)\right]. \quad [8.4b]$$

Methods were developed to derive the $\{K_A,\,\gamma_o,\,\delta_o\}$ values, and to determine the $\{g_m;\,m=(0,+M_F)\}$ and $\{c_m;\,m=(0,+M_F)\}$ constants from data. Whereas our *Initial Model* and *EIM* were $M_F = 0$ cases, the $M_F = 2$ case was used here to examine the Italy CoVID-19 data, as an *EOF* model example.

The *bing.com* data for Italy up to ~6/15/2020 was then analyzed, with **Figures 3-6** giving the new Italy results. Both the *EIM* and the *EOF* model provided good datafits, giving similar $N[t\rightarrow\infty]$ results for the final number of CoVID-19 pandemic cases, differing by only ~2% at the 1σ level.

The $\rho[t]$ post-peak behavior best indicates if a $\delta_o \neq 0$ model (CoVID-19 pandemic *Fast Shutoff*) is applicable. The $\delta_o \neq 0$ case likely is a second *Social Distancing* process, that operates along with, but is independent of the gradual pandemic *doubling time* changes. That *doubling time* change gives rise to a CoVID-19 pandemic *Slow Shutoff* ($\gamma_o \neq 0$), and that process still operates concurrently with the $\delta_o \neq 0$ CoVID-19 pandemic *Fast Shutoff*.

This analysis shows a wide variety of CoVID-19 data can be modeled using $\{K_A, \gamma_o, \delta_o, t_{offset}\}$ as parameters, covering: (I) an exponential rise at CoVID-19 pandemic start; (II) a gradual lengthening of *doubling times* for a pandemic *Slow Shutoff*; and (III) an exponential decay for pandemic *Fast Shutoffs*.

9 List of Figures

Figure 1: *Updated Initial Model for ITALY, CoVID-19 data to 6/15/2020.* Number of daily CoVID-19 cases calculated as if *Social Distancing* started at 3/2/2020, but only data from 3/10/20 actual *Social Distancing* start, with $N = 10,149$ cases, was used in calculations.

Figure 2: *Comparison of Initial Model Best-Fit to Measured Data.* Best-fit done on *Logarithmic Y-axis*, using data from 3/10/20 actual *Social Distancing* start with $N = 10,149$ cases, through 6/15/20 with $N = 237,290$.

Figure 3: *Enhanced Initial Model (EIM)* for ITALY CoVID-19 data to 6/15/20. *EIM* best fit with $N_A[t] \sim exp(-Z_A[t])$ using enhanced $Z_A[t]$ function having an exponential decay. Adding in exponential decay term gives significantly improved fit, compared to prior *OFM*.

Figure 4: *Enhanced Initial Model (EIM)* datafit for ITALY CoVID-19 data to 6/15/20. *EIM* best fit with $N_A[t] \sim exp(-Z_A[t])$ using enhanced $Z_A[t]$ function having an exponential decay. Datafit minimizing *rms* error on *Logarithmic Y-axis* gives significant improvement vs *OFM*.

Figure 5: *Enhanced Orthogonal Functions (EOF)* for ITALY CoVID-19 data to 6/15/20. Orthogonal functions give additional parameters for further datafit improvement, using a 3-term series ($M_F = 2$). Result shows *EIM*, by itself, provides most of the improvement.

Figure 6: *Enhanced Orthogonal Functions (EOF)* for ITALY CoVID-19 data to 6/15/20. Data for total number of CoVID-19 cases versus time, compared with 3-term *EOF* model for $N(Z_A[t])$ shows excellent match after *Social Distancing* start at $N = 10,149$.

10 References

1. https://www.MedRxiv.org/content/10.1101/2020.05.04.20091207v1, https://doi.org/10.1101/2020.05.04.20091207, "*Initial Model for the Impact of Social Distancing on CoVID-19 Spread*", Genghmun Eng.

2. https://www.MedRxiv.org/content/10.1101/2020.06.30.20143149v1, https://doi.org/10.1101/2020.06.30.20143149, "*Orthogonal Functions for Evaluating Social Distancing Impact on Covid-19 Spread*", Genghmun Eng

3. https://www.medrxiv.org/content/10.1101/2020.03.27.20043752v1, "*Forecasting COVID-19 impact on hospital bed-days, ICU-days, ventilator-days and deaths by US state in the next 4 months*", IHME COVID-19 Health Service Utilization Forecasting Team.

4. https://www.geekwire.com/2020/univ-washington-epidemiologists-predict-80000-covid-19-deaths-u-s-july/ "*Univ. of Washington researchers predict 80,000 COVID-19 deaths in U.S. by July*", Alan Boyle, *GeekWire*, March 26, 2020.

5. https://www.yahoo.com/finance/news/coronavirus-modelers-raise-projected-u-041641553.html, "*Coronavirus modelers raise projected U.S. death toll and lengthen state-by-state recovery timeline*", Alan Boyle, *GeekWire*, April 27, 2020.

6. https://covid19.healthdata.org, update of 29 April 2020.

7. http://www.healthdata.org/covid/updates "*COVID-19: What's New for May 4, 2020: Updated IHME COVID-19 projections: Predicting the Next Phase of the Epidemic*", IHME COVID-19 Health Service Utilization Forecasting Team.

8. https://finance.yahoo.com/news/pandemic-projection-puts-u-death-220824741.html, "*New pandemic projection puts U.S. death toll at nearly 135,000, due to less social distancing*", Alan Boyle, *GeekWire*, May 4, 2020.

9. www.bing.com/covid: '*Bing COVID-19 Tracker*', and https://www.bing.com/covid?form=CPVD07.

10. G. N. Watson, "*A Note of the Polynomials of Hermite and Laguerre*", Journal of the London Mathematical Society, **13**(1938), pp. 29-32.

11. J. Gillis and G. Weiss, "*Products of Laguerre Polynomials*", Math. Comput., **14**(69), Jan. 1960, pp. 60-63

12. For correct results, calculations done by *swp55.exe* requires **no** commas in the integer matrix or vector entries, when using: $Scientific Workplace^{TM}\_Compute\_EvaluateNumerically$. It is due to *swp55.exe* also accepting European notation where $10,149 \Leftrightarrow 10.149$.

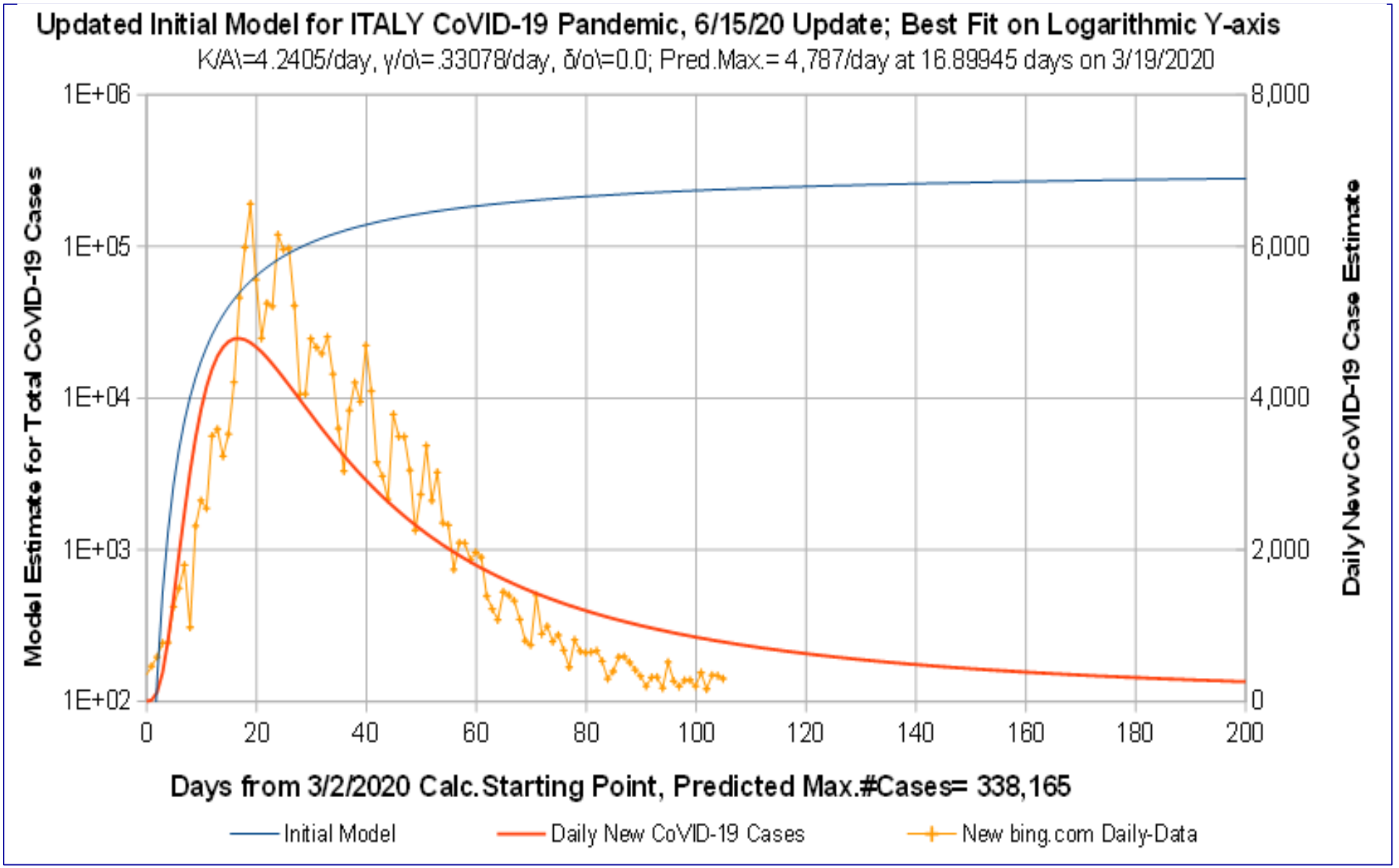

Figure 1: Updated *Initial Model* for ITALY, CoVID-19 data to 6/15/2020. Number of daily CoVID-19 cases calculated as if Social Distancing started at 3/2/2020, but only data from 3/10/20 actual *Social Distancing* start, with ***N=10,149*** cases, was used in calculations.

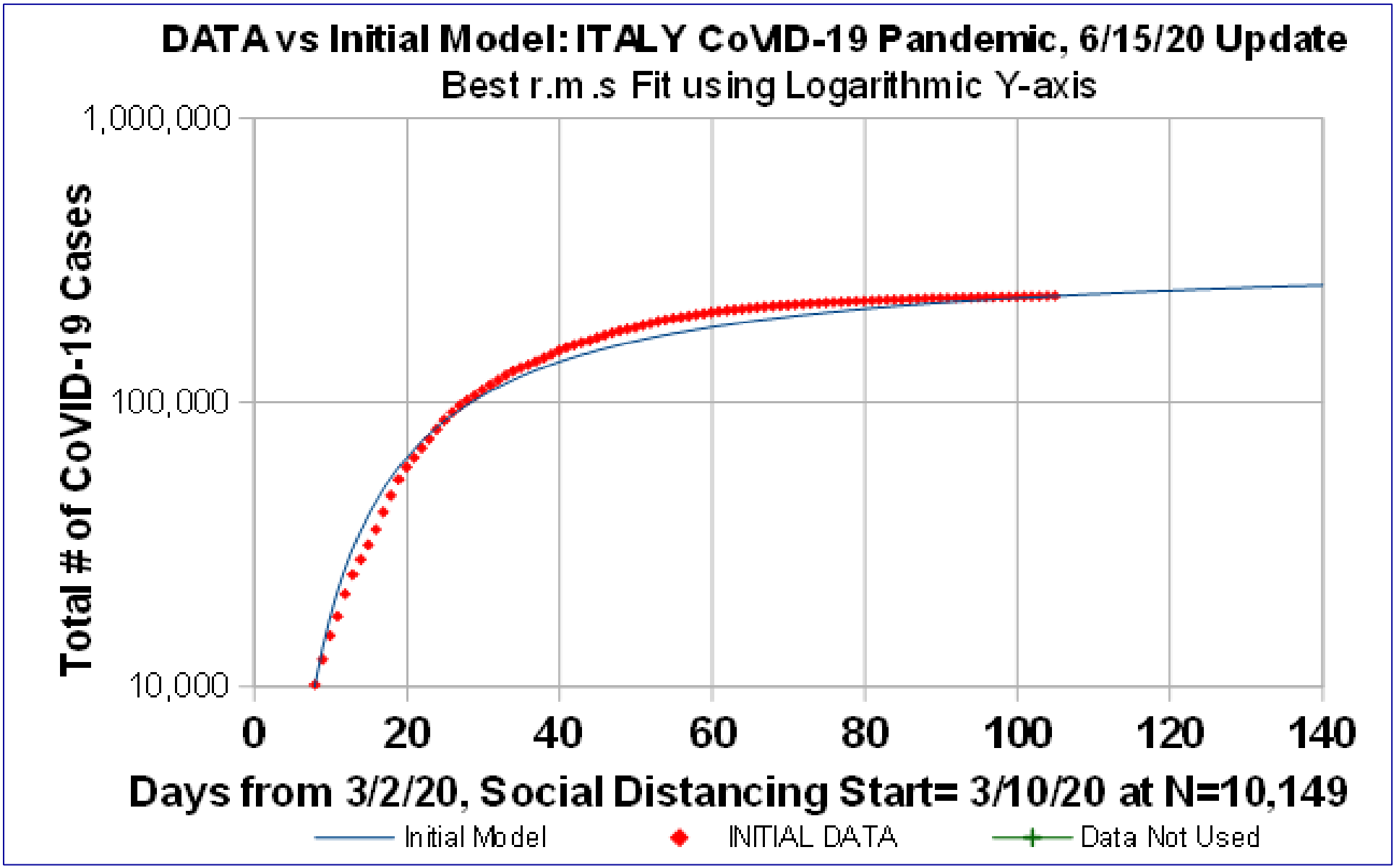

Figure 2: Comparison of *Initial Model* Best-Fit to Measured Data. Best-fit done on Logarithmic Y-axis, using data from 3/10/20 actual *Social Distancing* start with ***N=10,149*** cases, through 6/15/20 with ***N=237,290***.

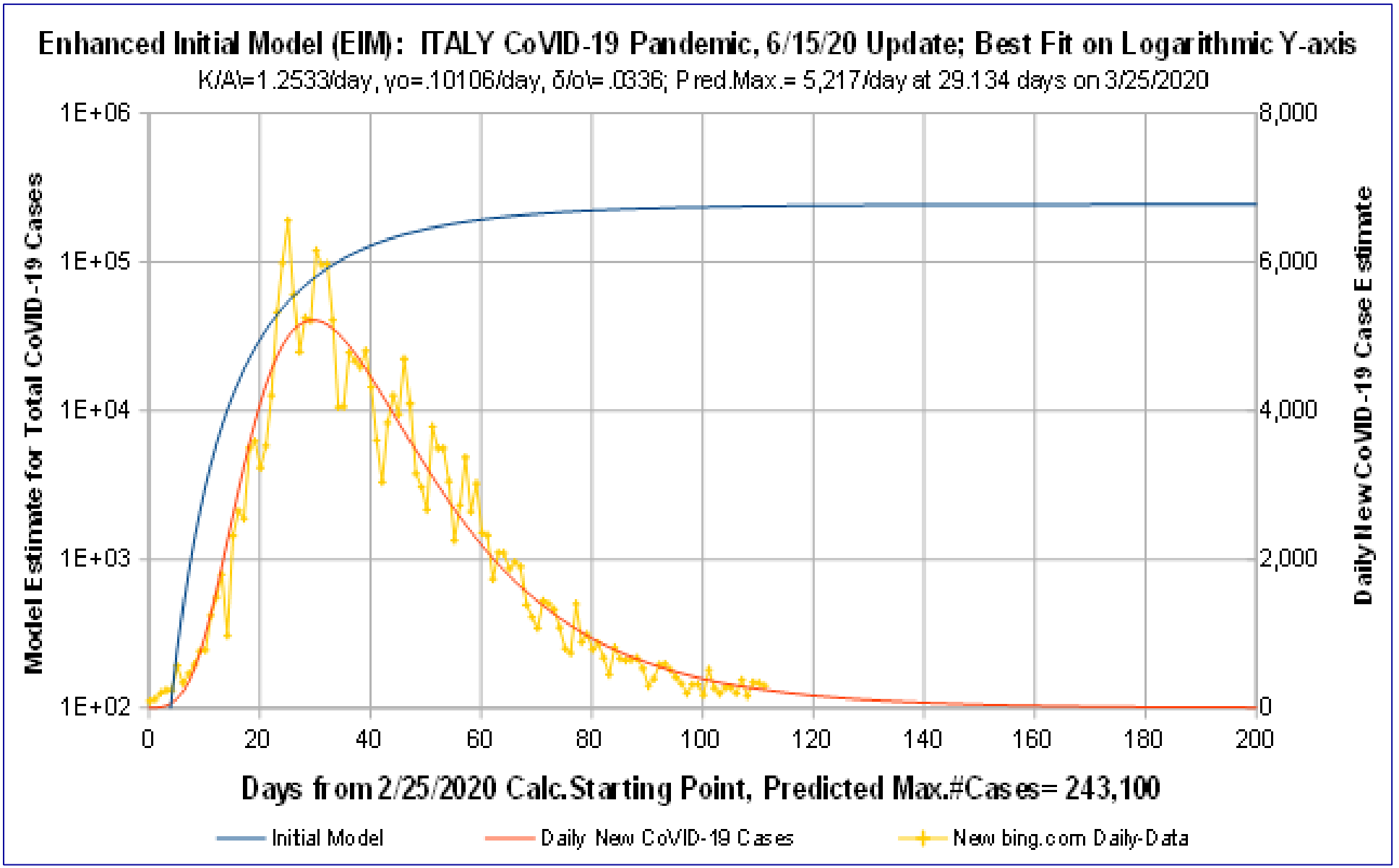

Figure 3: *Enhanced Initial Model (EIM)* for ITALY CoVID-19 data to 6/15/20.
EIM best fit with $N_A[t] \sim exp(-Z_A[t])$ using enhanced $Z_A[t]$ function having an exponential decay. Adding in exponential decay term gives significantly improved fit, compared to prior *OFM*.

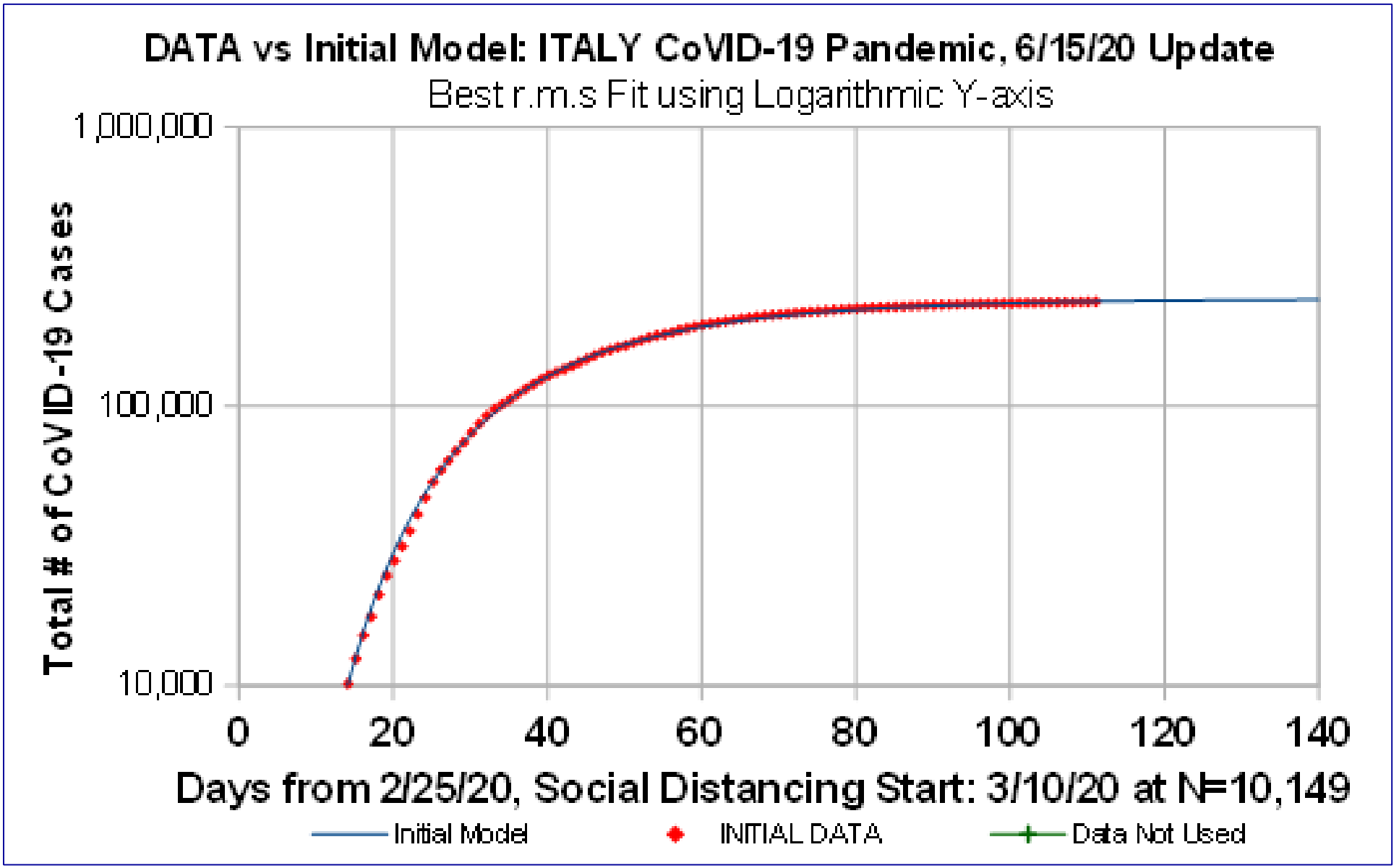

Figure 4: ***Enhanced Initial Model (EIM)*** **datafit for ITALY CoVID-19 data to 6/15/20.**
EIM best fit with $N_A[t] \sim \exp(-Z_A[t])$ using enhanced $Z_A[t]$ function having an exponential decay. Datafit minimizing *rms* error on *Logarithmic Y-axis* gives significant improvement vs *OFM*.

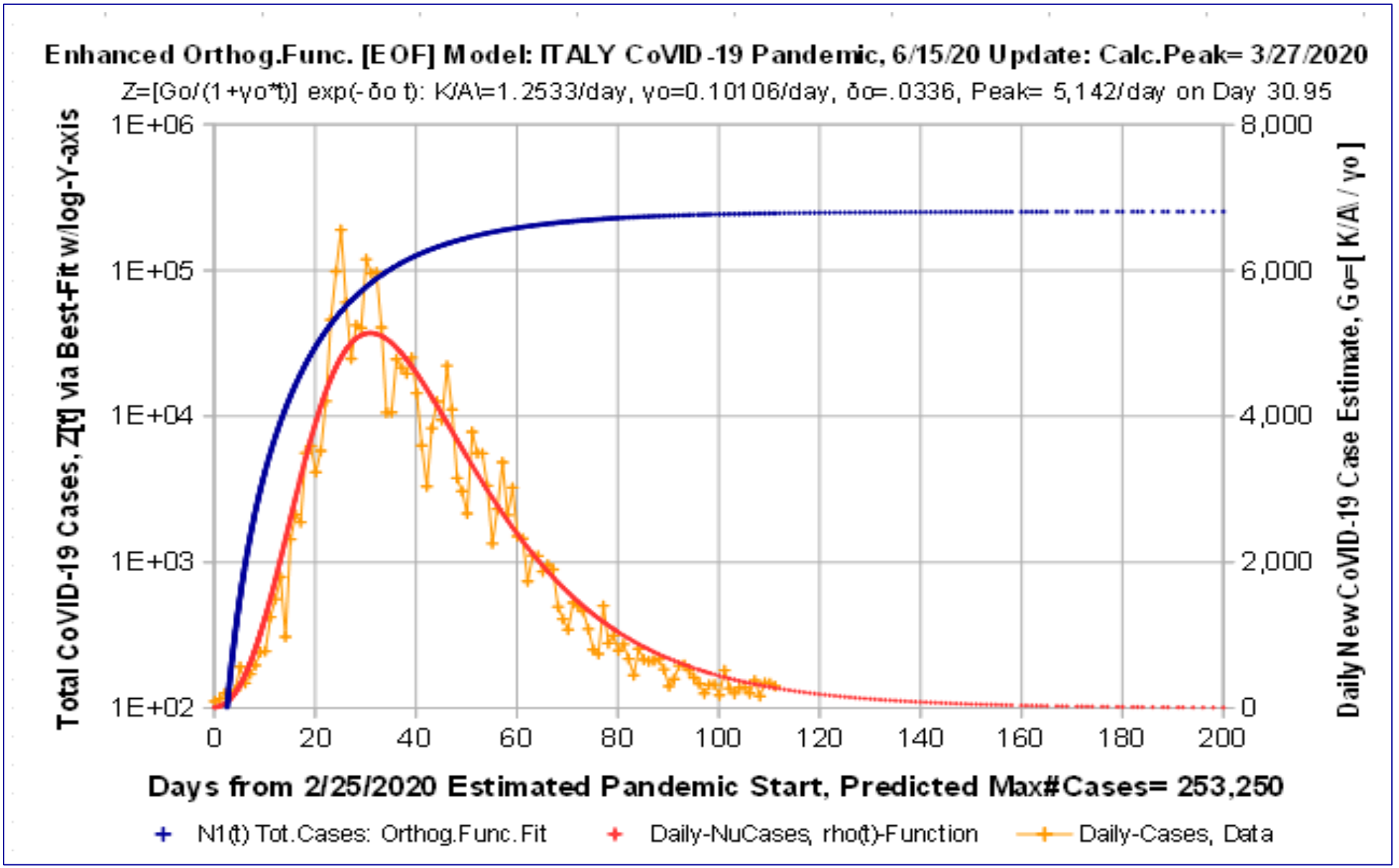

Figure 5: ***Enhanced Orthogonal Functions (EOF)*** **for ITALY CoVID-19 data to 6/15/20.** Orthogonal functions give additional parameters for datafit improvement, using a 3-term series ($M_F=2$). Result shows *EIM*, by itself, provides most of the improvement.

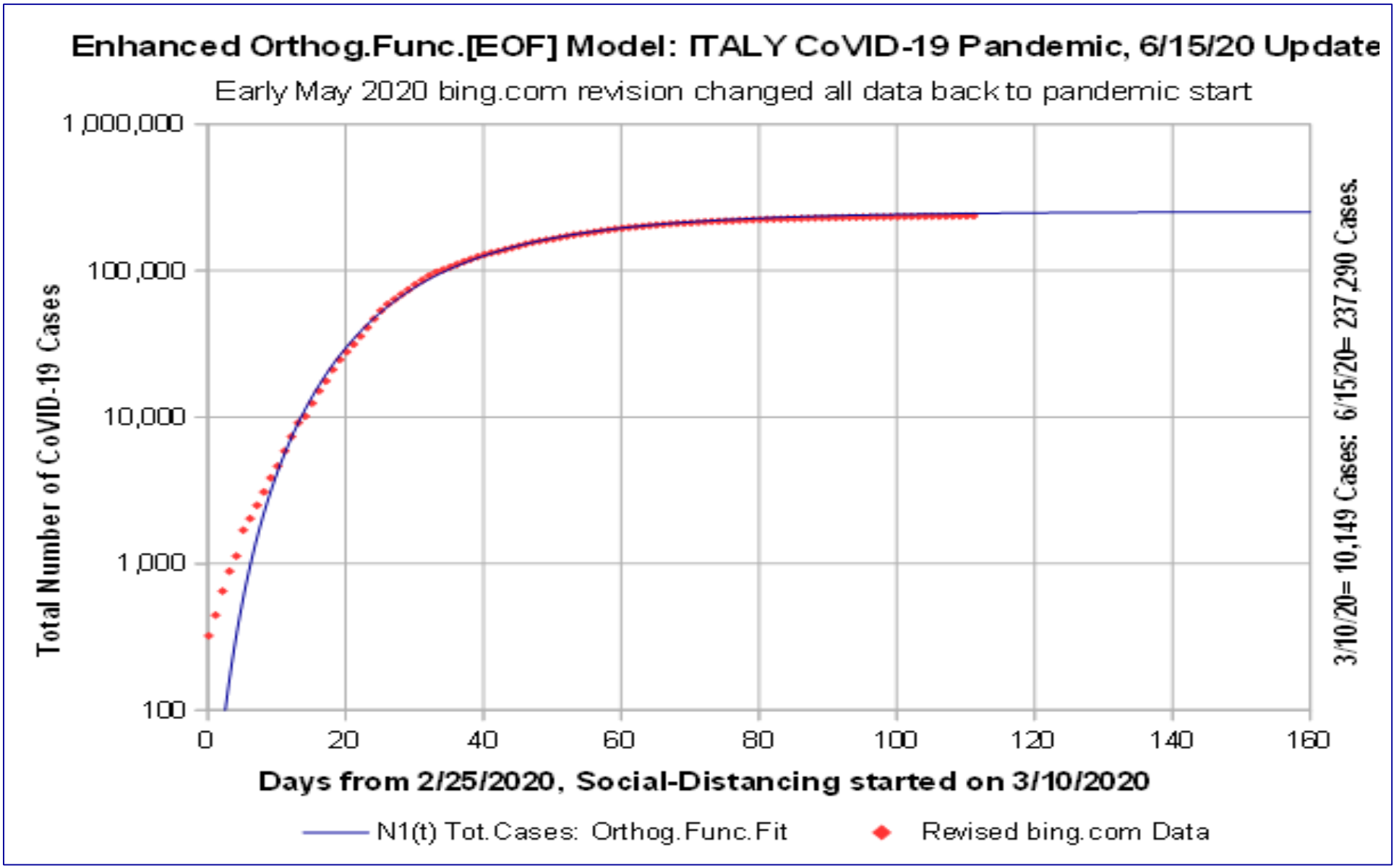

Figure 6: *Enhanced Orthogonal Functions (EOF)* for ITALY CoVID-19 data to 6/15/20. Data for total number of CoVID-19 cases versus time, compared with 3-term *EOF* model for $N(Z_A[t])$ shows excellent match after *Social Distancing* start at $N=10,149$.